Theoret. chim. Acta (Berl.) 31, 239—260 (1973)

Direct Calculation of Ionization Potentials of Closed-Shell Atoms and Molecules

Lorenz S. Cederbaum*.
Institut für Physikalische Chemie der Technischen Universität München

Received May 4, 1973

Vertical ionization potentials, electron affinities and information about quasi-particles can be obtained by using the technique of the single-particle propagator. The expansion of the self-energy part up to third order perturbation theory can be evaluated numerically, but does not lead, in most cases, to satisfying results. A theoretical and numerical analysis of the diagrammatic expansion of the self-energy part requires the introduction of a renormalized interaction and renormalized hole and particle lines.

Key words: Atomic and molecular structure – Electronic structure – Ionization – Many-body perturbation theory

1. Introduction

Many-body perturbation theories have been applied with success to nuclear structure [1], to high-density electron gas [2] and also to a wide range of other subjects as phonons, plasmons and superconductivity [3]. In addition, these theories have been also applied to atoms and molecules. In the case of atoms correlation energies [4, 5], dipole and quadrupole polarizabilities, shielding factors, transition probabilities [4], photodetachment cross sections [6], Fermi contact terms [7], open-shell SCF orbitals [29] and ionization potentials [5, 8] have been calculated. In the case of molecules the correlation problem [9], natural orbitals [30] and ionization potentials [10–12] have been treated (non semi-empirical calculations). The application of a many-body perturbation theory to ionization potentials is more than just an alternative for the usual calculation of these quantities, since Koopmans' defect [11], the difference between the ionization potential obtained by Koopmans' theorem [13] and the exact one, is calculated directly without subtracting large numbers of nearly equal magnitude.

In previous discussions in [14] and applications to atoms [5, 8] and molecules [10] the self-energy part has been expanded up to second order. Extensive calculations, however, have shown that, at least for small molecules, the expansion of the self-energy part up to second order is far from being able to reproduce the experimental results [11, 12, 15]. Therefore, a more elaborate form of perturbation theory has to be derived which is done in the following sections. Quantitative results are discussed for the nitrogen molecule. Further calculations for F_2, C_2H_2, H_2O and H_2CO are given in [15].

* Present Address: Physik-Department, Technische Universität München, Deutschland.

2. General Theory

In this section the general theory of Green's one-particle functions and of the self-energy part is discussed which is essential for the following sections.

In the following text we use the occupation number formalism in which the operators a_i and a_i^+ are the annihilation and the creation operators for a particle in the state $|i\rangle$ satisfying the anti-commutation relations

$$[a_i, a_j^+]_+ = \delta_{ij}, \quad [a_i, a_j]_+ = [a_i^+, a_j^+]_+ = 0, \qquad i \equiv (i, \sigma_i). \tag{2.1}$$

Let a system of N interacting fermions in the ground state be described by Ψ_0^N. In the Heisenberg representation the Green's one-particle function is defined by

$$G_{kk'}(t, t') = -i\langle \Psi_0^N | T\{a_k(t)\, a_{k'}^+(t')\} | \Psi_0^N \rangle, \qquad a_k(t) = e^{iHt} a_k e^{-iHt}, \quad a_k \equiv a_k(0), \tag{2.2}$$

T = Wick time-ordering operator.

The spectral representation can be written as

$$G_{kk'}(\omega) = \int_{-\infty}^{\infty} G_{kk'}(t, t')\, e^{i\omega(t-t')} d(t-t') \tag{2.3}$$

$$= \sum_l \frac{\langle \psi_0^N | a_k | \psi_l^{N+1} \rangle \langle \psi_l^{N+1} | a_{k'}^+ | \psi_0^N \rangle}{\omega + A_l + i\eta} + \sum_l \frac{\langle \psi_0^N | a_{k'}^+ | \psi_l^{N-1} \rangle \langle \psi_l^{N-1} | a_k | \psi_0^N \rangle}{\omega + I_l - i\eta}$$

$\eta \to 0^+$

where the relations

$$I_l = E_l^{(N-1)} - E_0^{(N)}$$
$$A_l = E_0^{(N)} - E_l^{(N+1)}$$

hold[1]. $E_0^{(N)}$ is the ground state energy of the N-electron system and $E_l^{(N-1)}$ and $E_l^{(N+1)}$ the energy of a l-th state of the $(N-1)$- and $(N+1)$-electron systems, respectively. Hence, the problem of calculating ionization potentials and electron affinities is equivalent to the problem of calculating the poles of the one-particle Green's functions. Putting the energies corresponding to the molecular geometry of the initial state for $E_l^{(N-1)}$ and $E_l^{(N+1)}$ the vertical ionization potentials (VIPs) and electron affinities (VEAs), respectively, are obtained. In order to compare them with the Franck-Condon maxima of the experimental ionization spectrum, they should be corrected for vibrational effects [16].

The Green's one-particle function can be expanded in the time representation by means of a perturbation theory which is described in detail in [17–19]. It is therefore not considered here. It should be noted that, starting out from the equations of motion for the Green's n-particle functions, an infinite coupled set of equations results [20]. The uncoupling of this set of equations yields the same result as the perturbation expansion of the Green's functions.

The perturbation series of the Green's function, however, does not have a form which allows the evaluation of its poles. On the other hand the Dyson equation in

[1] In order to simplify, the first ionization potential is denoted by I_0.

the ω-representation

$$\begin{aligned} \boldsymbol{G} &= \boldsymbol{G}^0 + \boldsymbol{G}^0 \boldsymbol{\Sigma} \boldsymbol{G}\,, \\ \boldsymbol{G}^{-1} &= \boldsymbol{G}^{0\,-1} - \boldsymbol{\Sigma} \end{aligned} \tag{2.4}$$

is especially appropriate for this purpose. The poles of $\boldsymbol{G}$ correspond to the zeros of the eigenvalues of $\boldsymbol{G}^{-1}$. In Eq. (2.4) the quantity Σ_{sm} is the self-energy part and $G^0_{kk'}$ is the free Green's function

$$\begin{aligned} G^0_{kk'}(t, t') &= -i\langle \Phi_0 | T\{a_k(t)\, a^+_{k'}(t')\} | \Phi_0 \rangle \\ &= \delta_{kk'}\, e^{-i h_k (t-t')} \begin{cases} -i & t > t', \quad k \notin \{\text{occ}\} \\ i & t \leqq t', \quad k \in \{\text{occ}\} \end{cases} \end{aligned} \tag{2.5}$$

where Φ_0 is the ground state eigenfunction of H_0 and $\{\text{occ}\}$ is the set of the orbitals occupied in this state.

For the above reason $\boldsymbol{\Sigma}$ shall be considered in more detail:

Let the Hamiltonian be given by

$$\begin{aligned} H &= H_0 + H_w\,, \\ H_0 &= \Sigma h_i a^+_i\, a_i\,, \\ H_w &= \tfrac{1}{2} \Sigma V_{ijkl}\, a^+_i\, a^+_j\, a_l a_k \end{aligned} \tag{2.6}$$

where

$$\begin{aligned} h_i &= \langle \varphi_i(1) | h(1) | \varphi_i(1) \rangle\,, \\ V_{ijkl} &= \langle \varphi_i(1)\, \varphi_j(2) | V(1,2) | \varphi_k(1)\, \varphi_l(2) \rangle \end{aligned} \tag{2.7}$$

are the matrix elements of the one-particle operator h and the two-particle operator V, respectively, and $\{\varphi_s\}$ is a complete set of one-particle wave functions. From the perturbation expansion of $\boldsymbol{G}$ and the Dyson equation we obtain the expansion of $\boldsymbol{\Sigma}$. The perturbation series of the Green's function and hence the expansion of the self-energy part is greatly simplified by the application of a well-known diagrammatic method. The following definitions hold:

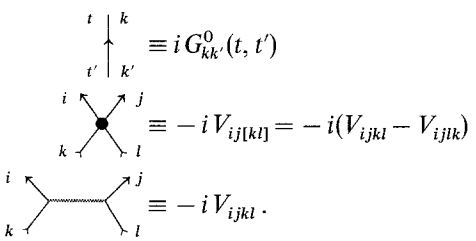

$$\equiv i\, G^0_{kk'}(t, t')$$

$$\equiv -i\, V_{ij[kl]} = -i(V_{ijkl} - V_{ijlk}) \tag{2.8}$$

$$\equiv -i\, V_{ijkl}\,.$$

The rules to draw the terms of a certain n-th order of the diagrammatic expansion of an element of $\boldsymbol{\Sigma}$ are:

(α1) The elements of each Graph are n $V_{ij[kl]}$-points and $(2n-1)$ G^0-lines. The elements of one kind can be connected only with elements of the other kind.

(α2) Graphs, which split into two graphs by removing a single G^0-line do not belong to $\boldsymbol{\Sigma}$ according to the Dyson equation.

(α3) All topologically not equivalent linked graphs with two free indices have to be drawn according to the rules (α1) and (α2).

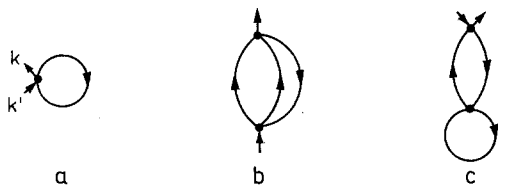

Fig. 1. The graphs of the first (a) and second (b, c) order of the expansion of Σ

In Fig. 1 the first and second order of the expansion are reported as an example.

The graphs which are obtained via (α1)–(α3) by replacing the $V_{ij[kl]}$-points by the wiggle are called Feynman graphs. Any of the graphs treated here contains several Feynman graphs, e.g.

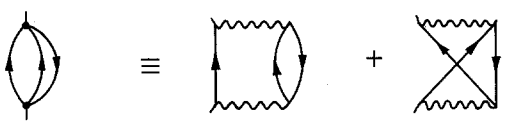

(2.9)

Except for the rules (β6) and (β7), all the following rules for evaluation of diagrams are also valid for Feynman diagrams.

(β1) Join the free indices k, k' of an n-th order diagram of the expansion of $\Sigma_{kk'}(t, t')$ with a $e^{i\omega(t-t')}$-line, which shall be denoted by

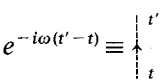

(β2) Draw the $(n-1)$ horizontal lines —·—·— between successive pairs of V-points according to:

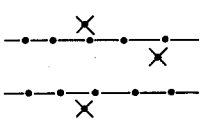

Any part of the diagram between two successive V-points is called a block.

(β3) Each G^0-line and $e^{-i\omega(t'-t)}$-line cut by a horizontal line supplies an additive contribution to the denominator of the block, namely:

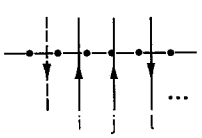

yields the dominator

$$+\omega - h_i - h_j + h_l + \cdots, \quad i, j \notin \{\text{occ}\}, l \in \{\text{occ}\}.$$

(β4) Multiply the interactions $V_{ij[kl]}$, the contributions of the blocks and a factor $(-1)^{\Sigma_l + \Sigma_s}$; then sum over the internal indices (Σ_l is the number of hole lines, Σ_s is the number of loops).

(β5) Each of the $n!$ time ordered diagrams has to be evaluated separately.

(β6) Each graphs has to be multiplied by 2^{-q} where q is the number of permutations of two G^0-lines in the diagram leaving the diagram unchanged (identity transformation).

(β7) The sign of the $V_{ij[kl]}$-points is not uniquely determined. The proper sign of the graph follows from a comparison with the sign of a Feynman graph which is contained in it.

As an example the terms for the graph of the second order of the expansion of $\Sigma_{kk'}(\omega)$ are obtained with the help of these rules.

$$\text{graph}(b) = \frac{1}{2} \sum_{\sigma_2,\sigma_3} \frac{V_{ks[fl]} V_{k's[fl]}}{\omega + h_s - h_f - h_l}; \tag{2.10}$$

$\sigma_2 = \{s \in \{\text{occ}\}; f, l \notin \{\text{occ}\}\}$, $\sigma_3 = \{s \notin \{\text{occ}\}; f, l \in \{\text{occ}\}\}$.

In the above perturbation theory the Hamiltonian of Eq. (2.6) has been used. Analogous results can also be obtained by choosing the perturbation H_w in a different way. In this work we choose now the Hartree-Fock operator

$$\begin{aligned} H_{\text{HF}} &= \Sigma \varepsilon_i a_i^+ a_i, \\ H_w &= \tfrac{1}{2} \Sigma V_{ijkl} a_i^+ a_j^+ a_l a_k - \Sigma \left(\sum_{l \in \{\text{occ}\}} V_{il[jl]} \right) a_i^+ a_j \end{aligned} \tag{2.11}$$

as the unperturbed operator H_0 and the canonical HF-orbitals as the one-particle wave functions φ_i. The ε_i are here the HF-energies. Very important reasons for this choice are the availability of HF calculations and that the HF-energies of occupied orbitals of closed-shell systems provide relatively good approximations for the VIPs. The absence of bound excited (unoccupied) HF states, as might be the case for neutral atoms, leads to a slow convergence of the perturbation expansion [21]. The convergence of the expansion for correlation energies of atoms was greatly improved by using the $V(N-1)$ potential of Kelly [4]. For closed-shell molecules, however, with many bound excited HF states we have no reason to assume a better convergence of the expansion of the self-energy part especially in calculating VIPs.

A consequent use of the $V(N-1)$ potential leads to a great expense for systems with many electrons since these excited states should be calculated in the potential field of $N-1$ *other* electrons [22] and therefore this potential is different for different excited states.

If the HF operator is taken to be H_0 then on account of the first term of H_w, graphs containing $G^0_{kk}(t, t+0)$-lines need no more be considered [18]. This means that only h_i has to be replaced by ε_i in the expressions for the graphs and that, in addition, the number of graphs shrinks considerably. Graph (b) is the only remaining graph in Fig. 1, hence Koopmans' theorem is obtained in the first order of the expansion. As already mentioned in the introduction the expansion of the self-energy part up to the second order is in many cases far from being able to reproduce the experimental results. Therefore we have to use a more elaborate form of perturbation treatment. A general way to do so is to renormalize quantities as the interaction, vertex and particle- and hole-lines. An example for a renormalized interaction is given by the random phase approximation (see Section 4.1). By the renormalization of hole- and particle-lines a transformation of G^0-lines into G-lines is understood. A graph, which is to be "dressed", is often referred to as "skeleton". By self-consistent perturbation theory we mean the self-consistent

solution of the equations

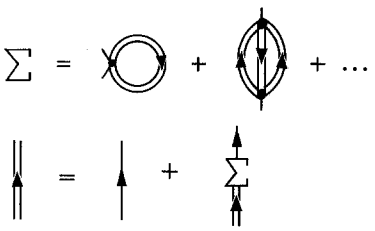

(2.12)

where the symbol

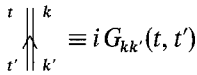

$$\equiv i G_{kk'}(t, t') \tag{2.13}$$

is used.

In all renormalizations attention must be paid to overcounting.

In the next section the pole strengths of the Green's functions are discussed and in Section 4 a self-energy part which is appropriate for calculating VIPs is derived. We use the nitrogen molecule as an example throughout this manuscript. Additional numerical calculations are given in [12, 15, 23].

3. Restriction to Low Energy; Main and Secondary Poles

In the following text some properties of the self-energy part which are essential for this work are mentioned. It should be noted that the self-energy part $\boldsymbol{\Sigma}$ also has poles. The following notation will be used: the poles of graph (b) in Eq. (2.10) with the index set σ_2 are denoted by $\Sigma_{+1}, \Sigma_{+2}, \ldots$ in the order of increasing energy and the poles with the index set σ_3 are denoted by $\Sigma_{-1}, \Sigma_{-2}, \ldots$ in the order of decreasing energy. The energy intervals (Σ_l, Σ_{l+1}), $l \neq -1$, will be denoted by the index l for $l \geqq 1$, by $l+1$ for $l \leqq -2$ and the interval $(\Sigma_{-1}, \Sigma_{+1})$ by $l = 0$. These definitions are illustrated in Fig. 2, where a schematic plot of $\Sigma_{ii}(\omega)$ is given.

In the picture of the Hartree-Fock quasiparticles the poles Σ_{-k} for $k \geqq 1$ correspond to processes in which one particle is separated and simultaneously another one is excited to an unoccupied orbital. In a similar manner the poles Σ_k for $k \geqq 1$ are connected with processes in which one particle is added and another one excited. It can be shown that exactly one pole of the eigenvalue $D_{ii}(\omega)$ of the Green's function $\boldsymbol{G}$ is situated between any two successive poles of the self-energy

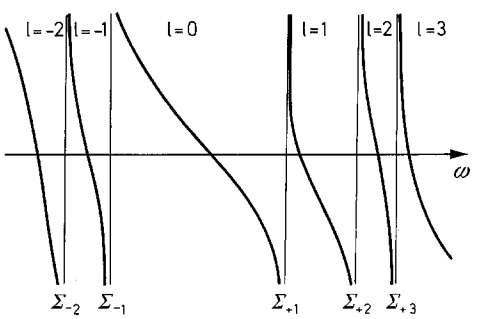

Fig. 2. A schematic plot of Σ_{ii} for the definition of its poles

part [12, 24]. This statement is easily verified for the second order of the perturbation expansion with the help of Eq. (2.10) [12]. An essential consequence of this statement is, that the zeros of the eigenvalue D_{kk}^{-1} of $\boldsymbol{G}^{-1}(\omega)$ which do not satisfy the conditions

$$\omega_k \in (\Sigma_{-1}, \Sigma_{+1}), \quad |\omega_k - \Sigma_{\pm 1}| \gg 0 \tag{3.1}$$

have to be treated in a different way than the zeros which do satisfy these conditions. The present work deals only with such solutions k of the Dyson equation which satisfy the above conditions. The remaining VIPs and VEAs are treated elsewhere [12, 24]. *A common theory for all* VIPs *and* VEAs *is developed in* [24] *but it leads to a great numerical expense.*

A perturbation expansion of the Green's one-particle function gives information not only about the energy values of the VIPs and VEAs but also about the utility of the one-particle picture for ionization and particle addition processes. The desired information is provided by the pole strengths of the Green's function, which are considered in the following. First of all, some definitions: P_{kl} is the pole strength of the k-th eigenvalue $D_k(\omega)$ of the Green's function matrix $\boldsymbol{G}$ to the pole in the interval l and a_{ijkl} is the pole strength of $G_{ij}(\omega)$ to the same pole (k, l).

$$\begin{aligned} P_{kl} &= \lim_{\omega \to \omega_{kl}} D_k(\omega) \cdot (\omega - \omega_{kl}), \\ a_{ijkl} &= \lim_{\omega \to \omega_{kl}} G_{ij}(\omega) \cdot (\omega - \omega_{kl}), \end{aligned} \tag{3.2}$$

ω_{kl} is the energy-coordinate of the pole and $S_{ikl} = S_{ik}(\omega_{kl})$ is an element of the eigenvector matrix $\boldsymbol{S}(\omega)$ to the same pole.

$$\boldsymbol{D}^{-1} = \boldsymbol{S}^{+} \boldsymbol{G}^{-1} \boldsymbol{S}. \tag{3.3}$$

By means of the Dyson equation one obtains directly for the pole strength

$$P_{kl}^{-1} = 1 - \frac{\partial}{\partial \omega} (\boldsymbol{\Sigma} + \boldsymbol{\varepsilon})_k \Big|_{\omega_{kl}} \tag{3.4}$$

where $\boldsymbol{A}_k$ means $(\boldsymbol{S}^{+} \boldsymbol{A} \boldsymbol{S})_{kk}$ generally.

In order to interpret the pole strengths one has to start out from their definition. By use of Eq. (2.3) one gets

$$\begin{aligned} &a_{iikl} = P_{kl} |S_{ikl}|^2 = |\langle \psi_{kl}^{N-1} | a_i | \psi_0^N \rangle|^2, \\ &k \in \{\text{occ}\}, l = 0, -1, -2, \ldots, \\ &k \notin \{\text{occ}\}, l = -1, -2, \ldots, \\ &1 \geqq a_{iikl} \geqq 0. \end{aligned} \tag{3.5}$$

$|\psi_{kl}^{N+1}\rangle$ and $|\psi_{kl}^{N-1}\rangle$ are true states of the $(N+1)$-particle system and $(N-1)$-particle system, respectively.

Hence, a_{iikl} is the probability to find the state $a_i|\psi_0^N\rangle$ in the state $|\psi_{kl}^{N-1}\rangle$, that means the projection of a true state on a fictive one. The result of "removing" a HF-particle from the true ground state is described by $a_i|\psi_0^N\rangle$, the true state after ionization is described by $|\psi_{kl}^{N-1}\rangle$. In case a_{iikl} is not much less than 1, the "removing" is nearly identical with the ionization.

Analogous conclusions are obtained for the pole strengths a_{iikl}, where

$$k \in \{\text{occ}\}, l = 1, 2, 3, \ldots,$$

$$k \notin \{\text{occ}\}, l = 0, 1, \ldots.$$

One has only to replace a_i by a_i^+, ψ_{kl}^{N-1} by ψ_{kl}^{N+1} and "removing" by "addition".

For the example of N_2 we calculated the following pole strengths:

$$P_{2\sigma_u,0} = 0.87,$$

$$P_{3\sigma_g,0} = 0.91,$$

$$P_{1\pi_u,0} = 0.94.$$

In order to compare those pole strengths of $\boldsymbol{D}$ with those of $\boldsymbol{G}$ we must know the values of S_{ikl}.

All numerical results indicate that the eigenvectors of $\boldsymbol{G}$ associated with eigenvalues ω_{kl} which have pole strengths, P_{kl}, not much less than 1, may be approximated very well by unit vectors. This is mainly due to the fact that the inequality

$$|(\varepsilon_i + \Sigma_{ii}) - (\varepsilon_j + \Sigma_{jj})| \gg |\Sigma_{ij}|, \quad i \neq j \tag{3.6}$$

is satisfied for all our examples.

The eigenvectors of $\boldsymbol{G}$ were calculated for the example of N_2 with the self-energy part in second order and are compiled in Table 1.

If the ionization is well described by the "removing" of a quasi-particle in the state k, then the corresponding Green's function in the range of the solution must show a similar form as the free function $G_{kk}^0(\omega)$: The self-energy part can be decomposed into imaginary and real part for real values of ω according to

$$\boldsymbol{\Sigma} = \boldsymbol{\Sigma}^R + \boldsymbol{\Sigma}^I. \tag{3.7}$$

Table 1. Eigenvectors of $\boldsymbol{G}^{-1}$ at $\omega = \omega_{k0}$ calculated with the self-energy part in second order for N_2. The basis-set used is described in [11]

Species	k							
	$2\sigma_g$	$2\sigma_u$	$1\pi_u$	$3\sigma_g$	$1\pi_g$	$3\sigma_u$	$4\sigma_g$	$2\pi_u$
$2\sigma_g$	0.9932	0	0	0.0346	0	0	0.0011	0
$2\sigma_u$	0	0.9995	0	0	0	−0.0031	0	0
$1\pi_u$	0	0	1.0000	0	0	0	0	0.0329
$3\sigma_g$	−0.1146	0	0	0.9990	0	0	0.0069	0
$1\pi_g$	0	0	0	0	1	0	0	0
$3\sigma_u$	0	−0.0121	0	0	0	0.9999	0	0
$4\sigma_g$	−0.0025	0	0	0.0050	0	0	0.9980	0
$2\pi_u$	0	0	0.0038	0	0	0	0	0.9995
$5\sigma_g$	0.0224	0	0	0.0265	0	0	0.0631	0
$4\sigma_u$	0	0.0294	0	0	0	−0.0146	0	0

Starting out from the Dyson equation and expanding $(\varepsilon+\Sigma^R)_k$ about $\omega_{kl}=(\varepsilon+\Sigma^R)_k|_{\omega_{kl}}$ to the linear term and expanding Σ_k^I about ω_{kl} to the constant term one obtains

$$D_k(\omega\approx\omega_{kl})=\frac{P_{kl}}{\omega-\omega_{kl}+i\tau_{kl}^{-1}}+f_{kl}(\omega\approx\omega_{kl})$$
$$\tau_{kl}^{-1}=P_{kl}\cdot\Sigma_k^I(\omega_{kl})\cdot\begin{cases}-1, & -\omega_{kl}=\text{VIP}\\ +1, & -\omega_{kl}=\text{VEA}\end{cases} \tag{3.8}$$

where $f_{kl}(\omega)$ is a correction function for the higher orders of the expansion about ω_{kl}. This expansion leads to the above result only if $\boldsymbol{S}$ is independent of $\boldsymbol{\Sigma}^I$ for $\eta\to 0^+$. But this is true, because $\boldsymbol{S}$ has no poles in the open interval between two successive poles of $\boldsymbol{\Sigma}$. Hence, if $f_{kl}(\omega\approx\omega_{kl})$ is unessential and $P_{kl}\approx 1$, then $D_k(\omega\approx\omega_{kl})$ has the form of a quasi-particle propagator. The corresponding quasiparticle has a finite life time τ_{kl}.

Equation (3.5) and the important relation

$$\sum_{k,l}a_{ijkl}=\delta_{ij}\,, \tag{3.9}$$

which is proved by removing the unit operators between the Heisenberg operators a_k and a_k^+, in Eq. (2.3), imply, that, if D_k takes the form of a quasi-particle propagator, there is only one dominant pole strength, P_{kl} for each eigenvalue D_k of $\boldsymbol{G}$. This pole shall be referred to as main pole, the remaining poles shall be called secondary poles. The properties of the secondary poles are treated extensively elsewhere [12, 24].

4. Inclusion of Higher Orders

The expression for the graph of the second order of the expansion of the self-energy part has already been given as an example in Section 2. All numerical calculations for Ne, N_2, F_2, H_2O, C_2H_2 and CO_2 [11, 12, 15, 25] show uniquely that the expansion of the self-energy part to the second order does not at all suffice to evaluate the VIPs via the Dyson equation. As an example the VIPs of N_2 calculated with the self-energy part of second order are compiled in Table 2.

For the above one cannot expect that taking in account the third order will be sufficient. An evaluation of additional orders turns out to be completely useless, as the number and the magnitude of the expressions go up explosively with the

Table 2. Results for the three lowest ionizations of N_2. R2 = VIP calculated with self-energy part in second order. RF = VIP calculated with the present theory. All energies in eV

Species	Exp. VIP [28]	R2	RF
$2\sigma_u$	18.78	17.00	18.59
$1\pi_u$	16.98	16.96	16.83
$3\sigma_g$	15.60	14.44	15.50

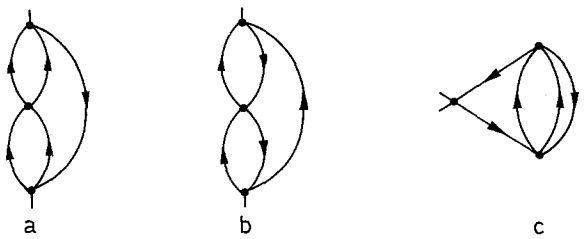

Fig. 3. The graphs of third order of the expansion of Σ

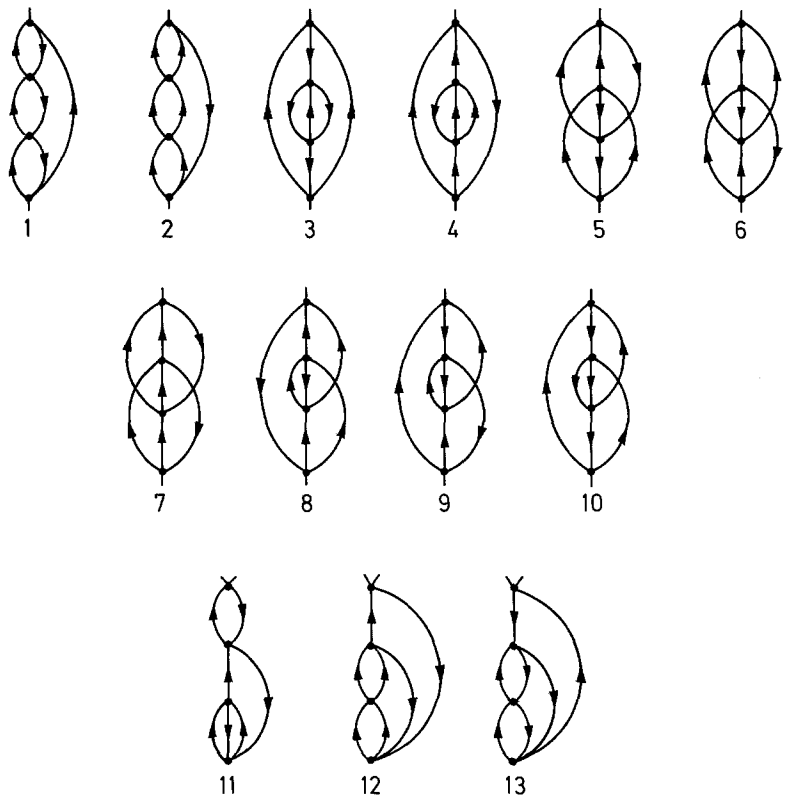

Fig. 4. The graphs of fourth order of the expansion of Σ

order of the expansion. The graph of the second order contains already 4 terms with 3 indices each. The graphs of the third order reported in Fig. 3 contain 84 terms with 5 indices each. One notes, however, that these graphs can still be calculated numerically. The necessary numerical methods are described elsewhere [12, 15]. The graphs of the fourth order, reported in Fig. 4, contain already 3120 expressions with 7 indices each. Therefore it is not possible to evaluate the total fourth order numerically.

One has to find out which graphs yield the important contributions, and then to calculate or, at least, to estimate these to infinite order.

As a first step towards the solution of this problem it is reasonable to investigate the essential results of the solid-state physics and nuclear physics with respect to their application in atomic and molecular physics.

4.1. *A Short Comparison with Electron Gas and Nuclear Matter*

It is common in the treatment of metals to introduce a scaling parameter r_s describing the volume per electron in an electron gas. It can be shown that, in the high-density case ($r_s \to 0$), the sum of the ring diagrams ("RPA")

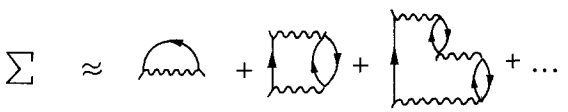

(4.1)

describes the self-energy part sufficiently well [26, 19]. With r_1 denoting the Bohr radius the volume per electron in the electron gas is

$$\Omega_e = \frac{4\pi}{3}(r_s \cdot r_1)^3 . \tag{4.2}$$

Let R_n be the radius of the n-th Bohr orbit and N_{eff} the number of electrons considered, then from

$$R_n \approx n^2 \cdot r_1 \cdot Z_{\text{eff}}^{-1} \tag{4.3}$$

it follows that:

$$r_{s_n} \approx n^2 Z_{\text{eff}}^{-1} N_{\text{eff}}^{-1/3} . \tag{4.4}$$

In regard of the inner electrons with $Z_{\text{eff}} \gg 1$ the relation $r_s \ll 1$ follows from Eq. (4.4). Thus, it is reasonable to evaluate the correlation energy for such atoms by means of a model of a high-density non-uniform electron gas. Considering only the outer-shell electrons on the other side, one obtains, e.g. for phosphorus $r_s \approx 1.3$. Therefore, the approximation of the self-energy part by ring diagrams does not work well in evaluating VIPs of atoms and especially not of molecules. It should be mentioned here that Brueckner [27] already tried to evaluate correlation energies of atoms with the help of a model of a high-density non-uniform electron gas. He obtained the important result that it has no sense to consider the atom as an uniform high-density electron gas and that the density gradient does not converge in the case of inhomogenity.

For the treatment of nuclear matter, however, circumstances are different. As before, it is also here common to introduce a parameter similar to r_s. With a standing for the effective range of the interaction and r_0 standing for the average distance between the interacting particles one speaks of low-density, if $r_0/a \gg 1$. Galitzki [26] showed that each hole line in a graph of the self-energy part is associated with a factor a/r_0. The sum of the graphs containing only one hole line

which are called ladder graphs, dominates in the low density case.

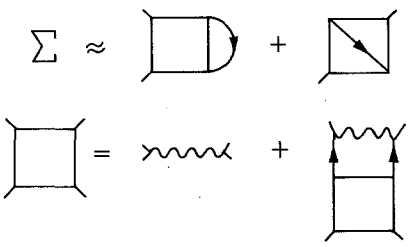

(4.5)

Theoretical as well as numerical comparisons of

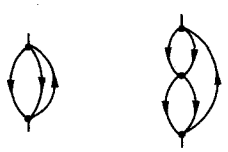

(4.6)

and

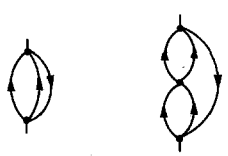

(4.7)

show, however, that, for atoms and molecules, the contribution of the first mentioned graphs are comparable with those of the second mentioned graphs and, as a rule, even exceed them [12].

All these considerations lead to the result that atoms and molecules are located in the region between intermediate density and high-density, *which means in a region, where it cannot be expected that just a few graphs dominate. This renders a reasonable evaluation of the self-energy part much more difficult.*

4.2. *Antigraphs and Renormalized Interaction*

All graphs of third order and a number of graphs of fourth order have been evaluated for the systems Ne, N_2, F_2, H_2O, CO_2, C_2H_2 and H_2CO. The contributions of some of these graphs were of the same order of magnitude as the contributions of the graphs of second order. If we assume the convergence of the perturbation expansion, some of the graphs must compensate each other at least partly. This is confirmed by numerical results. The assumption that the contributions of the single graphs go down with increasing order of the expansion cannot be maintained. Hence, it is useless to consider as many graphs of a certain order of the expansion as possible without closer examination. It should be examined whether there exists a small "parameter" which gives us an idea how to select the important terms in the expansion of Σ. In order to do so first of all some of the specific features of graphs of third order are considered in more detail. Each graph is split into its 6 time orders where the nomenclature given in Fig. 5 will be used.

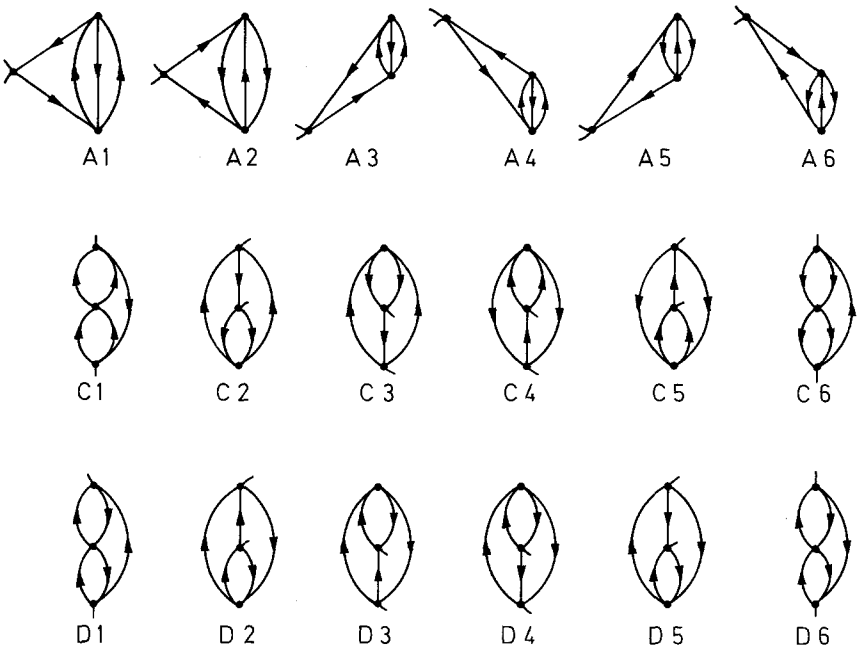

Fig. 5. The notation of the time ordered graphs of third order

In the following only diagonal elements of the self-energy part of third and higher orders are considered (see Section 3). It is easily shown, that, for $i=j$ the relations

$$\begin{aligned} A3 &= A4, A5 = A6, \\ X2 &= X3, X4 = X5, X = C, D \end{aligned} \tag{4.8}$$

hold. There remain 12 different time ordered graphs.

It is rather difficult to determine additional *exact* relations, if it is possible at all. Expressing the terms of the graphs $C1 - C6$ and $A1 - A6$ in an appropriate way facilitates relations as, e.g.

$$\begin{aligned} &|C1| \ll |C6| \qquad \omega \approx \varepsilon_k, k \in \{\text{occ}\} \\ &A1, C6 < 0 \\ &A2, C1 > 0 \end{aligned} \quad \text{for all } k. \tag{4.9}$$

As one can see from the explicit expressions, it is difficult to build up relations for $D1 - D6$ and between D and C graphs, as the D-graphs contain 8 expressions each, which cannot be collected as easily as for the C-graphs. Only simple relations like

$$D1 < 0, D6 > 0 \qquad \omega \approx \varepsilon_k \tag{4.10}$$

may be established [12].

In order to determine additional relations among the graphs we make the approximation that the most important contributions to Σ arise from one occupied

Table 3. The contributions of the graphs of third order for N_2 [eV][a]

Orb.	$A1$	$A2$	$2.A3$	$2.A5$	$C1$	$D1$	$2.C2$	$2.D2$	$2.C4$	$2.D4$	$C6$	$D6$
$2\sigma_u$	−1.78	1.73	0.41	−0.39	0.10	−0.13	0.29	−0.25	−0.10	−1.79	−2.35	2.10
$3\sigma_g$	−1.70	1.77	0.42	−0.44	0.15	−0.16	0.35	−0.25	−0.12	−1.23	−1.56	1.34
$1\pi_u$	−1.80	1.77	0.44	−0.41	0.32	−0.30	0.77	−0.64	−0.08	−0.11	−0.61	0.65
$1\pi_g$	−1.76	1.39	0.38	−0.39	0.27	−0.46	0.03	0.16	−0.63	0.66	−0.40	0.32
$3\sigma_u$	−1.16	1.10	0.11	−0.11	0.21	−0.19	0.03	0.33	−0.03	0.04	−0.03	0.03
$4\sigma_g$	−1.35	1.27	0.17	−0.17	0.29	−0.27	0.02	0.36	−0.03	0.04	−0.02	0.02
$2\pi_u$	−1.52	1.40	0.22	−0.23	0.54	−0.68	0.18	0.07	−0.05	0.07	−0.04	0.04
$5\sigma_g$	−1.70	1.52	0.31	−0.29	1.04	−1.20	0.09	0.66	−0.12	0.11	−0.08	0.07

$\Sigma_{-1} = -37.90$ eV, $\Sigma_{+1} = 24.86$ eV.

[a] Each graph has been evaluated at $\omega =$ main pole.

orbital and one unoccupied orbital of suitable symmetry. With this approximation we deduce relations which are confirmed by a large number of numerical results. As well *ab initio* calculations for the above mentioned systems as semi-empirical HF-calculations for a larger number of molecules [25, 23] were available. The graphs of third order have been calculated in all these cases. As an example, the data of these graphs for the nitrogen molecule are compiled in Table 3. The numerical and theoretical results indicate that the following relations are valid:

$$\begin{gathered} 0 \geqq A1 \approx -A2, 0 \leqq C1 \approx -D1 \\ 0 \geqq C6 \approx -D6, A3 \approx -A5, \\ C2 \approx -D2 \qquad k \in \{\text{occ}\} \\ C4 \approx -D4 \qquad k \notin \{\text{occ}\} \end{gathered} \tag{4.11}$$

for

$$\omega \approx \omega_{k0}\,, \qquad |\omega - \Sigma_{\pm 1}| \gg 0\,.$$

Hence, there exist pairs of graphs distinguishing themselves by nearly compensating each other. Such graphs shall be referred to as antigraphs. Although they do not completely compensate each other, both together have to be considered as one quantity in the perturbation theory. In third order there exist 5 different pairs of antigraphs.

With $\chi_j^{(n)}$ and $g_k^{(n)}$ standing for a pair of antigraphs and an arbitrary graph of n-th order which is no antigraph, respectively, the self-energy part can be written:

$$\Sigma_{ii}(\omega) = \sum_{j_n, n} [\chi_{j_n}^{(n)}]_{ii} + \sum_{k_n, n} [g_{k_n}^{(n)}]_{ii}\,. \tag{4.12}$$

Both time ordered diagrams of the self-energy part of second order may be considered as antigraphs, too, since

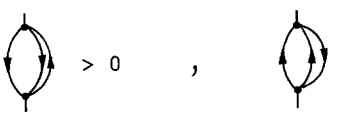

(4.13)

$$\omega \approx \omega_{k0}$$

hold.

This pair of antigraphs of second order, $\chi_1^{(2)}$, is essential for most orbitals and

$$|[\chi_1^{(2)}]_{ii}| \gg |[\chi_s^{(3)}]_{ii}|, \quad s = 1, 2, 3, 4, 5 \tag{4.14}$$

is valid for these orbitals, which indicates that the first sum converges quickly and can be estimated quite well by summing up to third order. Therefore, if the graphs of third order are calculated explicitly, then only graphs $\{g_{k_n}^{(n)}\}$, for $n \geqq 4$, have to be considered. We try to take account of the essential contributions of these graphs by introducing a time dependent effective interaction and renormalized hole- and particle-lines. The renormalized interaction shall be symbolized by

$$= -iV_{\text{eff}}(t, t'). \tag{4.15}$$

This renormalized interaction contains all graphs beginning with two free indices at the time t' and ending with two free indices at the time t:

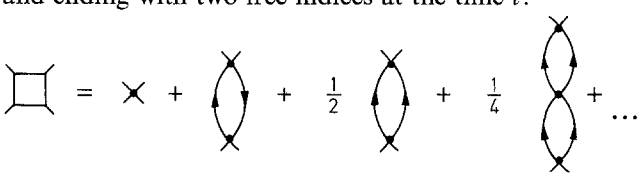

(4.16)

In this equation the factor of rule ($\beta 6$) in Section 2 is explicitly put in front of the graph.

It is evident, that the renormalized interaction satisfies the recurrence formula

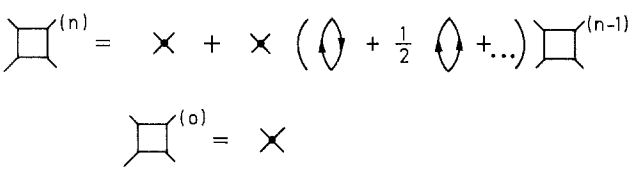

(4.17)

Numerical results prove that the calculation of V_{eff} by use of Eq. (4.17) converges slowly. It is useless, for this reason, just to evaluate a few orders and it is, therefore, necessary to estimate the rest.

Substituting the interaction by the renormalized one and paying attention to repetitions of graphs one gets in second order

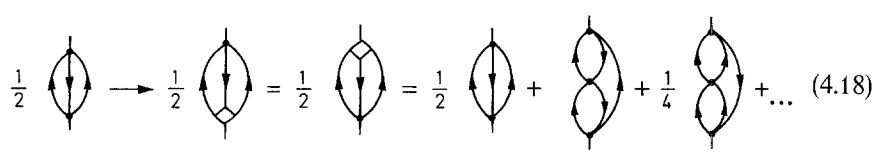

(4.18)

All ω-dependent graphs of third order as well as the graphs (1) and (2) in Fig. 4 are contained in the renormalized graph of second order.

Analogously

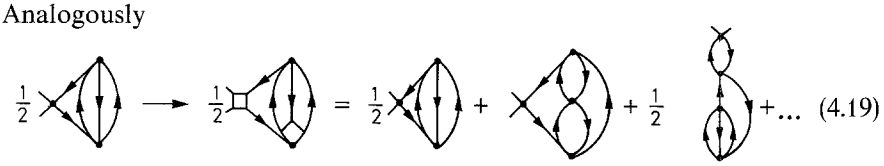

(4.19)

By use of the antigraph hypothesis one obtains

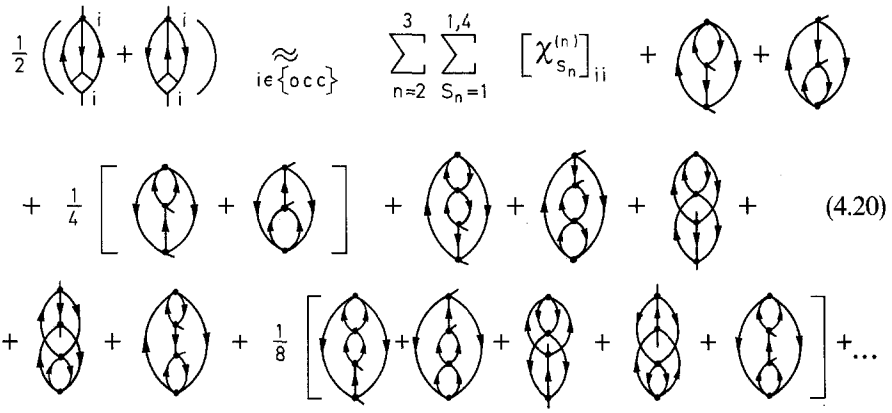

(4.20)

for the renormalized graph. It means, that graphs which arise from the graphs of third order which are not antigraphs are considered.

For $i \notin \{\text{occ}\}$ an analogous expression results [12]. It must be observed, however, that the error of the estimation arises in the fourth order, because *all ω-dependent graphs of third order are considered explicitly* in Eq. (4.20).

All drawn graphs on the right hand side of Eq. (4.20) are of the type $g_{k_n}^{(n)}$. These graphs have been numerically evaluated for all above examples and provide extremely large contributions [12, 15].

In the following we want to try to evaluate the renormalized graph of second order.

First, we have to make use of the fact that the following series are equal:

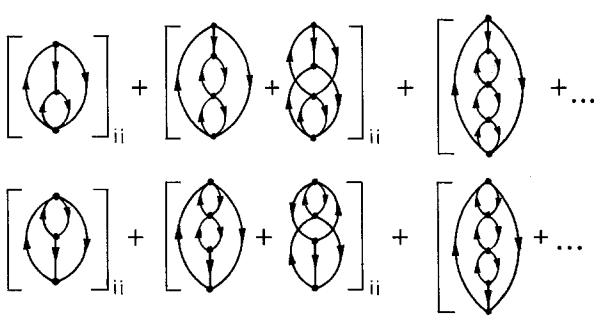

(4.21)

analogously

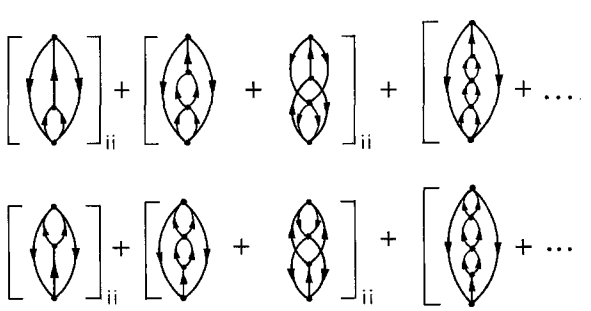

(4.21a)

In crude approximation these series may be estimated by geometric series. The quotient of the first two terms of the series in Eq. (4.21) and the series in Eq. (4.21a) shall be referred to as $q_i^{(a)}$ and $q_i^{(b)}$, respectively.

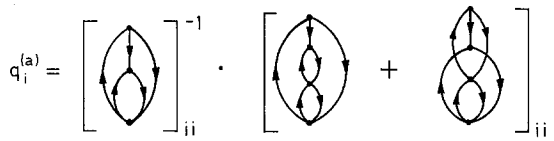

(4.22)

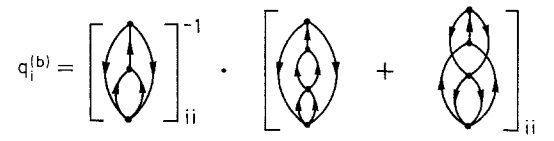

(4.22a)

In order to estimate the renormalized graph in Eq. (4.20) the graphs

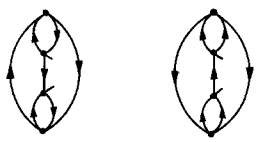

(4.23)

are left, which give only small contributions to the examples considered. But this must be checked for each new example.

For the example of N_2 the quotients $q^{(a)}$ and $q^{(b)}$ are:

$$q^{(a)}_{2\sigma_u} = -0.89, \quad q^{(a)}_{1\pi_u} = -0.99, \quad q^{(a)}_{3\sigma_g} = -0.87,$$
$$q^{(b)}_{2\sigma_u} = -0.30, \quad q^{(b)}_{1\pi_u} = -0.50, \quad q^{(b)}_{3\sigma_g} = -0.33.$$

This means that, as $C4$ yields only a small contribution, the contribution of the effective interaction is approximately given by the terms of second order and the half of $2 \cdot D4$.

The graph of second order is the first graph of the expansion, which depends on ω. The constant graph C in Fig. 3 is the first graph which does not depend on ω. Renormalizing this graph according to Eq. (4.19) one obtains in fourth order the ω-dependent graphs

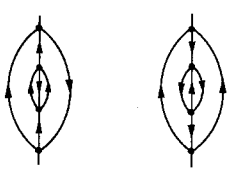

(4.24)

These graphs have a special meaning which is explained in the next section.

The graphs in Eq. (4.19) which do not depend on ω, are not of importance unless the corresponding antigraph relations in Eq. (4.11) are not satisfied sufficiently (Appendix A).

4.3. *Self-Consistent Perturbation Theory*

In Section 4.2 a renormalization of the interaction has been described. Numerical calculations show that the obtained results for VIPs are largely improved by

considering the renormalization. For further improvement we also consider the renormalization of hole- and particle-lines. The renormalization of the "skeleton" ⟲ is reduced to the HF-problem by use of Eq. (2.11) with

(4.25)

If we choose but the self-energy part of second order for a skeleton for the self-consistent perturbation theory, the calculation contains the graphs:

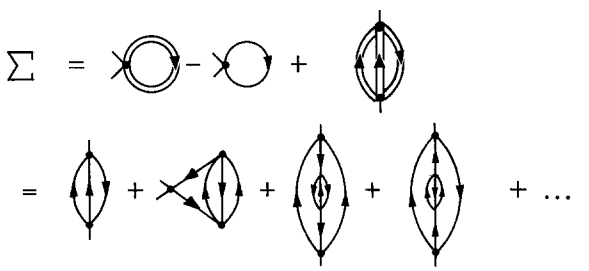

(4.26)

This becomes evident, if the single iteration steps are carried out by use of Eq. (4.26) and the diagrammatic Dyson equation (2.12).

By noting $G_{ij}(t, t')$ according to Eqs. (2.2) and (2.3), the renormalized graphs in the ω-space may be given straightforwardly by the use of the rules of Section 2 [12]. The expressions for the graphs are more simplified and better illustrated by starting out from a different consideration described in the following.

The characteristic equation

$$\boldsymbol{G}^{0-1}|\varphi_i\rangle = 0\,; \qquad |\varphi_i\rangle = \begin{pmatrix} 0 \\ \vdots \\ 1_i \\ \vdots \\ 0 \end{pmatrix} \tag{4.27}$$

is renormalized:

$$\boldsymbol{G}^{-1}|\varphi_{kl}\rangle = 0\,; \qquad |\varphi_{kl}\rangle = C_{kl}\Sigma S_{ikl}|\varphi_i\rangle\,. \tag{4.28}$$

C_{kl} being an arbitrary constant for the moment. The new "one-particle" functions $\{\varphi_{kl}\}$ are not orthogonal. Choosing

$$|C_{kl}|^2 = P_{kl} \tag{4.29}$$

and considering Eqs. (3.9) and (3.5), one obtains the completeness relation

$$\sum_{k,l} |\varphi_{kl}\rangle\langle\varphi_{kl}| = 1\,. \tag{4.30}$$

Hence, $\{\varphi_{kl}\}$ is a set of functions well adapted for the description of the renormalizing process $\boldsymbol{G}^0 \to \boldsymbol{G}$. Starting out from the skeleton we can describe the renormalization by very simple rules:

Only internal indices are transformed and following transformation properties hold:

$$k \in \{\text{occ}\} \to (k, l) = \begin{cases} k \in \{\text{occ}\}, & l = 0, -1, -2, \ldots \\ k \notin \{\text{occ}\}, & l = -1, -2, \ldots \end{cases}$$

$$k \notin \{\text{occ}\} \to (k, l) = \begin{cases} k \in \{\text{occ}\}, & l = 1, 2, 3, \ldots \\ k \notin \{\text{occ}\}, & l = 0, 1, \ldots \end{cases}$$

$$\begin{aligned} &\varepsilon_k,\ k \in \{\text{occ}\}, \to -I_{kl} \\ &\varepsilon_k,\ k \notin \{\text{occ}\}, \to -A_{kl} \end{aligned} \tag{4.31}$$

$$V_{stkf} = \langle \varphi_s(1)\varphi_t(2)|V(1,2)|\varphi_k(1)\varphi_l(2)\rangle \to \langle \varphi_{sl}(1)\varphi_{tl'}(2)|V(1,2)|\varphi_{kl''}(1)\varphi_{fl'''}(2)\rangle$$

$$= (P_{sl}P_{tl'}P_{kl''}P_{fl'''})^{1/2} \sum S_{isl}S_{jtl'}S_{ukl''}S_{qfl'''}V_{ijuq} \equiv \overline{V}_{\substack{stkf \\ ll'l''l'''}}.$$

The self-energy part given in Eq. (4.26) can be directly expressed:

$$\Sigma_{ij} = \sum_{\sigma} (\overline{V}_{\substack{ikjk \\ l\ l}} - \overline{V}_{\substack{ikkj \\ l\ l}})$$

$$+ \sum_{\sigma_1} \frac{(\overline{V}_{\substack{ij'kf \\ l\ l''l'}} - \overline{V}_{\substack{ij'fk \\ l\ l'l''}}) \cdot \overline{V}_{\substack{jj'kf \\ l\ l''l'}}}{\omega - I_{j'l} + A_{fl'} + A_{kl''}} + \sum_{\sigma_2} \frac{(V_{\substack{ij'kf \\ l\ l''l'}} - \overline{V}_{\substack{ij'fk \\ l\ l'l''}}) \overline{V}_{\substack{jj'kf \\ l\ l''l'}}}{\omega - A_{j'l} + I_{fl'} + I_{kl''}}. \tag{4.32}$$

The sets of indices σ, σ_1, σ_2 are to be taken from Eq. (4.31). As the self-consistent calculation of Eq. (4.32) is numerically too lengthy, it cannot be carried out without additional simplifications. By use of a finite number of unoccupied orbitals the sets of indices go up with the number of iteration steps. If the one-pole approximation is well satisfied (Section 3), we may write

$$\Sigma_{ij}^{(2)} \approx \sum_{\substack{k,f \in \{\text{occ}\} \\ j' \notin \{\text{occ}\}}} \frac{P_{j'}P_kP_f(V_{ij'kf} - V_{ij'fk})\,V_{jj'kf}}{\omega - A_{j'} + I_k + I_f} \tag{4.33}$$

$$+ \sum_{\substack{k,f \notin \{\text{occ}\} \\ j' \in \{\text{occ}\}}} \frac{P_{j'}P_kP_f(V_{ij'kf} - V_{ij'fk})\,V_{jj'kf}}{\omega - I_{j'} + A_k + A_f}.$$

P_s being the pole strength of a main pole. The introduction of the one-pole approximation for the graph of first order yields the simple relation

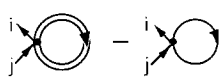

$$\approx \sum_{k \in \{\text{occ}\}} V_{ik}\,[jk]\,(P_k - 1) \tag{4.34}$$

The numerical evaluation of this relation leads to small differences between big numbers. In order to get rid of this inaccurateness *all constant graphs of third*

order are to be calculated explicitly. Nevertheless, an interesting conclusion can be deduced from Eq. (4.34): the contribution of these graphs in the one-pole approximation is negativ for $i=j$.

For the example of nitrogen the self-consistent calculation with the self-energy part given in Eq. (4.33) only slightly improves the results. The final results of the present perturbation theory for the VIPs of N_2 are reported in Table 2.

7. Summary

The method of the Green's functions provides a new approach to the calculation of ionization potentials and electron affinities. Moreover, it makes it possible to investigate one-particle properties of the system. An integral equation relating the Green's functions with the self-energy part gives us freedom to collect certain graphs to infinite order with the help of the perturbation expansion of the self-energy part to finite order. The problem to evaluate the Green's functions has hence been reduced to an investigation of the graphs of the self-energy part.

Expanding the self-energy part to the first order of perturbation theory yields Koopmans' theorem. Already in the second order of the perturbation expansion additional poles of the Green's functions are obtained, which cannot be explained by Koopmans' theorem. These ionization potentials correspond to ion states the expansion of which in terms of electron configurations contains mainly such configurations which differ by more than one orbital from the configuration describing the ground state of the initial molecule in the one-particle picture. VIPs of this type and VIPs in their energy region are not considered here, but have been investigated and calculated elsewhere [12]. Here, only these poles of the Green's functions are investigated which are situated far from the poles of the self-energy part.

In order to find these poles, first of all the second order of the self-energy part has been taken into account [10–12]. The numerical results, however, *prove that the second order is far from being able to reproduce the experimental results.* By going over to the *third order the results were improved,* but then it was evident that it is useless to evaluate only a finite number of orders.

Theoretical considerations and numerical calculations revealed that it is *necessary to introduce an effective interaction as well as renormalized particle- and hole-lines* in order to estimate the contributions of the graphs of higher orders.

Applications: As mentioned above, the theory has been applied to closed-shell molecules successfully [11, 12, 15]. For open-shell systems the theory may be applied as well, but the question, if the approximations, used here, are reasonable, has still to be investigated.

One of the main advantages of this perturbation treatment, compared with the calculation of the total energies of the corresponding states, is that only a small correction term has to be calculated and therefore less accurate wavefunctions are sufficient to obtain satisfactory results. It is already shown that in most cases reasonable values for Koopmans' defect can be calculated even with semiempirical CNDO-wavefunctions [23, 25].

Appendix A

For some examples the antigraph relation $A3 \approx -A5$ is not as well satisfied as the other relations in Eq. (4.11). In case the contribution of $A3 + A5$ is considerable, ω-independent graphs have to be taken into account for the calculation of

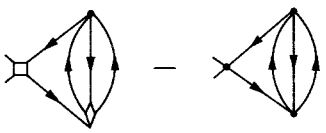

(A1)

The estimation of these graphs may be performed analogously to the evaluation of the renormalized graph of second order.

Acknowledgement. I would like to thank the Deutsche Forschungsgemeinschaft for financial support, the Leibniz-Rechenzentrum of the Bavarian Academy of Sciences for the necessary computing time and Prof. Dr. G. Hohlneicher for helpful discussions.

References

1. Brueckner, K.A., Gammel, J.L.: Phys. Rev. **109**, 1023 (1958). — Brueckner, K.A., Masterson, Jr., K.S.: Phys. Rev. **128**, 2267 (1962)
2. Gell-Mann, M., Brueckner, K.A.: Phys. Rev. **106**, 364 (1957)
3. e.g., Schultz, T.D.: Quantum field theory and the many-body problem. New York: Gordon and Breach 1964. — Schrieffer, J.R.: Theory of superconductivity. New York: Benjamin 1964. — Schrieffer, J.R.: In: Phonons and phonon interactions, Ed. Bak Thor. New York: Benjamin 1964
4. Kelly, H.P.: Phys. Rev. **136**, B896 (1964)
5. Doll, J.D., Reinhardt, W.P.: J. Chem. Phys. **57**, 1169 (1972). — Reinhardt, W.P., Doll, J.D.: J. Chem. Phys. **50**, 2767 (1969)
6. Cahse, R.L., Kelly, H.P.: Phys. Rev. A **6**, 2150 (1972)
7. Chang, E.S., Pu, R.T., Das, T.P.: Phys. Rev. **174**, 1 (1968)
8. Reinhardt, W.P., Smith, J.B.: J. Chem. Phys. **58**, 2148 (1973)
9. Miller, J.H., Kelly, H.P.: Phys. Rev. A **4**, 480 (1971)
10. Cederbaum, L.S., Hohlneicher, G., Peyerimhoff, S.: Chem. Phys. Lett. **11**, 421 (1971)
11. Cederbaum, L.S., Hohlneicher, G., v. Niessen, W.: Chem. Phys. Lett. **18**, 503 (1973)
12. Cederbaum, L.S.: Thesis, T. U. München 1972
13. Koopmans, T.: Physica **1**, 104 (1933)
14. Ecker, F., Hohlneicher, G.: Theoret. chim. Acta (Berl.) **25**, 289 (1972)
15. Cederbaum, L.S., Hohlneicher, G., v. Niessen, W.: Mol. Phys., in press
16. Meyer, W.: Inter. J. Quantum Chem. S **5**, 341 (1971)
17. Abrikosov, A., Gor'kov, L., Dzyaloshinskii, J.: Quantum field theoretical methods in statistical physics. Oxford: Pergamon Press 1965
18. Thouless, D.J.: The quantum mechanics of many-body systems. New York: Academic Press 1961
19. Mattuck, R.D.: Feynman diagrams in the many-body problem. London: McGraw-Hill 1967
20. Migdal, A.B.: Theory of finite Fermi systems and applications to atomic nuclei. London: John Wiley & Sons 1967
21. Kelly, H.P.: Phys. Rev. **131**, 684 (1963)
22. Kelly, H.P.: Phys. Rev. **144**, 39 (1966)
23. Kellerer, B., Cederbaum, L.S., Hohlneicher, G.: to be published
24. Cederbaum, L.S.: Mol. Phys., in press
25. Kellerer, B.: Thesis, T. U. München 1973

26. Pines, D.: The many-body problem. New York: Benjamin 1961
27. Brueckner, K. A.: Advan. Chem. Phy. **14**, 215 (1969)
28. Turner, D., Baker, C., Baker, A. B., Brandle, C.: Molecular photoelectron spectroscopy. London: Wiley-Interscience 1970
29. Albat, R., Gruen, N.: J. of Phys. B**6**, 601 (1973)
30. Albat, R.: Z. Naturforsch. **27**a, 545 (1972)

Dr. L. S. Cederbaum
Physik-Department der
Technischen Universität München
Theoretische Physik
8046 Garching bei München
Reaktorgelände
Federal Republic of Germany